Effects of beam pointing instability on two-beam interferometric lithography

Yongfa Fan, Anatoly Bourov, Michael Slocum Bruce W. Smith
Rochester Institute of Technology, Microelectronic Engineering Department
82 Lomb Memorial Drive, Rochester, NY 14623

ABSTRACT

In a photolithographic system, the mask patterns are imaged through a set of lenses on a resist-coated wafer. The image of mask patterns physically can be viewed as the interference of the plane waves of the diffraction spectrum captured by the lens set incident on the wafer plane at a spectrum of angles. Two-beam interference fringe is the simplest format of the image. Consequently, two-beam interferometric lithography is often employed for photolithographic researches. For two-beam interferometric lithography, beam pointing instability of the illumination source can induce fringe displacement, which results in a loss of fringe contrast if it happens during the exposure. Since some extent of beam pointing instability is not avoidable, it is necessary to investigate its effects on the contrast of the interference fringe. In this paper, the effects of beam pointing instability associated with a two-beam interferometric lithography setup are analyzed. Using geometrical ray tracing technique and basic interference theory, the relationship between the beam tilt angle and interference fringe displacement is established. For a beam pointing instability with random distribution, the resulted fringe contrast is directly proportional to the Fourier transform of the pointing distribution evaluated at $\frac{1}{2\pi}$. The effect of a pointing instability with normal distribution on interference contrast is numerically investigated.

Key words: Interferometric lithography, vibration, laser pointing instability

1. INTRODUCTION

In a conventional lithographic imaging system, the patterns on the mask are projected through a set of lenses on a wafer coated with photoresist where the image of the patterns is recorded.[1] Interference lithography produces periodic patterns in a photoresist film by the interfering of two coherent laser beams.[2-3] For a few special cases, diffraction-limited projection imaging is analogous to interference imaging. The first case is the projection imaging of a phase shifting grating mask (1:1 duty ration, alternating 180º phase shift, 100% transmission) with coherent illumination. The grating's 0th diffraction order is zero. If the pitch of the grating is such that only the ±1st diffraction orders are captured in the entrance pupil, the resulting image is simply the interference fringes of two plane waves with oblique angle θ (half of the angle subtended by the lens at the image plane). The second case is the projection imaging of a 1:1 binary grating mask with coherent illumination. If the pitch of the grating is such that only the 0th and ±1st diffraction orders are captured in the entrance pupil, the resulting image is the interference fringes of three plane waves, two beams with oblique angle θ, one normal to the image plane. The third case is the projection imaging of a 1:1 binary grating mask with off-axis coherent illumination. If the pitch of the grating is

such that only the 0th and one of the ±1st diffraction orders are captured in the entrance pupil, the resulting image is the interference fringes of two plane waves of different amplitudes with oblique angle θ (since the amplitude of the 0th order is different from that of the ±1st orders). For the above cases with partial coherence illumination, the resulting images still can be considered as interference fringes but with weaker ±1st diffraction orders since only part of the ±1st orders is captured in the entrance pupil. In a word, imaging of the above grating objects from an optical projection system can be reduced to the problems of plane wave interference.

The resemblance of projection imaging to interference imaging in the cases analyzed in the preceding paragraph has stimulated studies of optical projection systems using an interferometric setup.[4-8] Although those are special cases, they represent a system's resolution limits, which mostly define the system's capability. An advantage of using an interferometric setup is that the costly lenses are not needed. At the same time, a single interferometric setup possesses the flexibility of emulating lenses with various numerical apertures. The polarization of beams can be conveniently manipulated, allowing study of polarization effects. An extra flexibility is that the relative amplitude of the beams can be easily controlled.

In a research or a fabrication environment, there are many factors which can contribute to laser beam direction fluctuation, such as laser intrinsic pointing instability, mechanical resonant vibration, environmental vibration, etc. All those factors can be lumped as one parameter: beam pointing instability. A typical laser with a beam pointing stability of 20 μrad [9] could cause a beam shift of 2μm after propagating a distance of 10 cm. Considering that interferometric lithography together with immersion techniques is capable of printing sub-30 nm line/space patterns, a beam shift of 2μm is an immense number. Therefore, it is necessary to analyze the effects of beam pointing instability on the contrast of the interferometric fringe used for lithography. In this paper, a simple geometrical ray tracing technique and the basic interference theory are applied to relate beam tilt angle with interference fringe displacement, which induces fringe contrast loss. The relationship will provide a good understanding of how the interference fringe is affected beam pointing instability.

2. THEORETICAL MODEL

A schematic of two-beam interferometric lithography system is shown in Figure 1. The laser beam, after expansion, polarization and spatial filtering, is split by a phase-shifting grating into a series of discrete diffraction orders. With the residual 0^{th} order and other higher orders being blocked, the $\pm 1^{st}$ orders are directed at oblique angles toward a wafer coated with resist. Tilting of the beam during the exposure could blur the interference fringe. However, it should be noted that not every mode of beam direction tilt necessarily blurs interference fringe. Only beam tilt that causes fringe displacement (i.e. the change of the phase of the sinusoidal wave) will cause blurring, as is illustrated in Figure 2. In this experimental setup, a beam tilt in the grating perpendicular direction could cause fringe displacement. In this section, the phase shift of the interferometric fringe will be analyzed as a function of beam tilt angle, as well as a function of the setup configuration parameters.

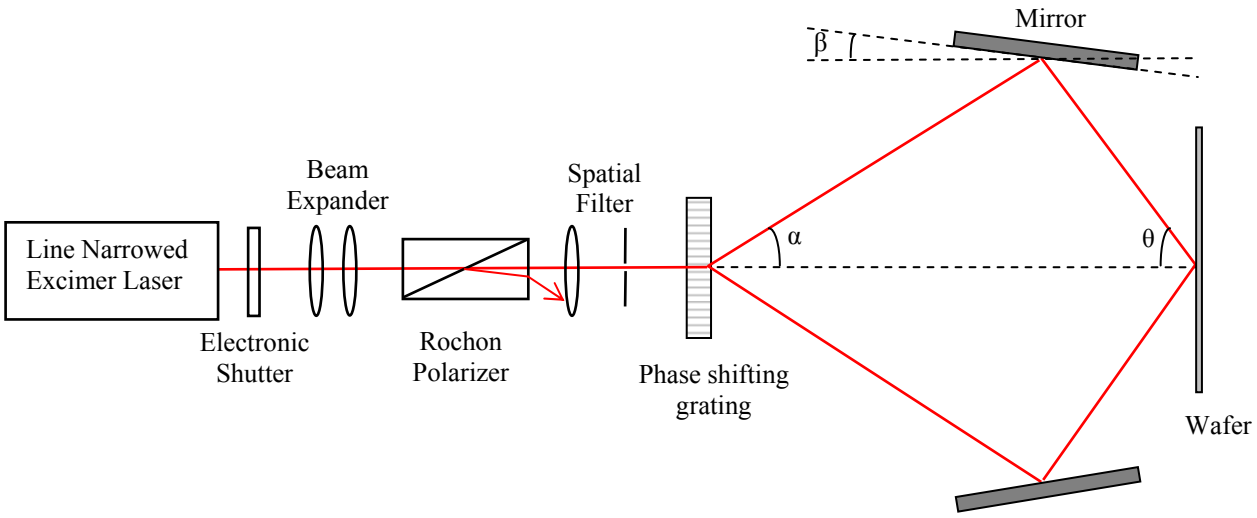

Figure 1. Schematic of interferometric lithography setup.

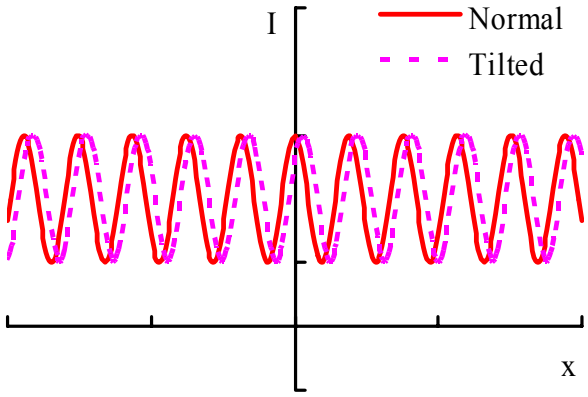

Figure 2. Interference fringe from tilted beam is displaced relative to that from normal beam, causing fringe blurring.

A schematic illustrating laser beam tilt in the experimental setup is shown in Figure 3. A normal incident beam is split by the phase grating into various diffraction orders, the $\pm 1^{st}$ orders of which are redirected to interference at the wafer plane. The diffraction angle of the first orders is defined by,

$$\sin\alpha = \frac{\lambda}{p} \qquad [1]$$

To achieve an interference angle θ at the wafer plane, a mirror tilt angle of β is required,

$$\beta = \frac{\theta - \alpha}{2} \qquad [2]$$

D is defined as the normal distance to the setup central axis from the point where the center of the beam hits the mirror. For a given grating pitch p and a required interference angle θ, the mirror separation (2D) describes the size of the setup.

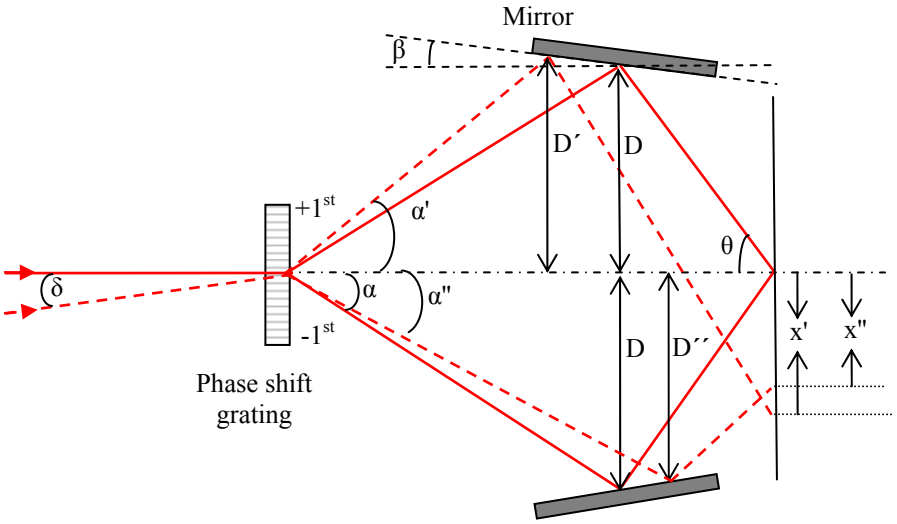

Figure 3. A schematic showing laser beam tilt. The solid beam is normal and the dashed beam is tilted by an angle of δ. The parameters used in the calculation are labeled in the figure.

Assume that the beam incident on the grating is tilted by an angle δ relative to normal due to beam pointing instability, then the diffraction angles of the first orders can be expressed by grating equation as,

$$\sin\alpha' = \frac{\lambda}{p} + \sin\delta \qquad [3]$$

$$\sin\alpha'' = \frac{\lambda}{p} - \sin\delta \qquad [4]$$

where α' and α'' are the $\pm 1^{st}$ diffraction orders respectively. For the $+1^{st}$ order, now the center of the beam hits the mirror at a different point, from which the normal distance to the central axis, D' is related to D in the following equation,

$$D'\cot(\alpha') + (D'-D)\cot(\beta) = D\cot(\alpha) \qquad [5]$$

Rearrangement of the above equation gives.

$$D' = \frac{D\cot(\alpha) + D\cot(\beta)}{\cot(\alpha') + \cot(\beta)} \qquad [6]$$

The beam travel distance L', from the grating, reflected by the mirror to the wafer plane can be derived as,

$$L' = \frac{D'}{\sin(\alpha')} + \frac{D[\cot(\alpha) + \cot(\theta)] - D'\cot(\alpha')}{\cos(\theta')} \qquad [7]$$

where θ' is the incident angle to wafer normal, $\theta' = \alpha' + 2\beta$. The titled beam insects with the wafer plane at a location which is x' from the central axis,

$$x' = \frac{D[\cot(\alpha) + \cot(\theta)] - D'\cot(\alpha')}{\cot(\theta')} - D' \quad [8]$$

Similarly, the following relationships can be derived for -1st order beam:

$$D''\cot(\alpha'') - (D - D'')\cot(\beta) = D\cot(\alpha) \quad [9]$$

$$D'' = \frac{D\cot(\alpha) + D\cot(\beta)}{\cot(\alpha'') + \cot(\beta)} \quad [10]$$

$$L'' = \frac{D''}{\sin(\alpha'')} + \frac{D[\cot(\alpha) + \cot(\theta)] - D''\cot(\alpha'')}{\cos(\theta'')} \quad [11]$$

$$x'' = D'' - \frac{D[\cot(\alpha) + \cot(\theta)] - D''\cot(\alpha'')}{\cot(\theta'')} \quad [12]$$

where $\theta'' = \alpha'' + 2\beta$. The double prime symbols denote the correspondent parameters for the -1st order beam.

With all those, the optical path distance between the ±1st orders on the wafer plane at the central axis can be expressed as,

$$\begin{aligned} OPD &= n[(L' - x'\sin(\theta')) - (L'' + x''\sin(\theta''))] \\ &= n[L' - x'\sin(\theta') - L'' - x''\sin(\theta'')] \end{aligned} \quad [13]$$

where n is the refractive index of the media. The corresponding phase difference is,

$$\begin{aligned} \phi &= \frac{2\pi}{\lambda} OPD \\ &= \frac{2\pi n}{\lambda}[L' - x'\sin(\theta') - L'' - x''\sin(\theta'')] \end{aligned} \quad [14]$$

Equation [14] is the basic equation that relate beam tilt angle with the phase shift of the resultant interference fringe. From this equation, the corresponding displacement of the fringe can be found, and subsequently the contrast loss. In section 3, the phase shift is analyzed as a function of various configuration parameters. In section 4, the effect of beam tilt with a statistical distribution is analyzed.

3. ANALYSIS OF BEAM TILT USING THE MODEL

The phase shift due to beam tilt versus beam tilt angle is plotted in Figure 4. A grating pitch of $p = 600\,nm$, setup size of $D = 1\,cm$, interference angle of $\theta = 45°$, and source wavelength of $\lambda = 193\,nm$ are used in the calculation. It is shown that a beam tilt of 1° will cause a phase shift of π, which is the worst case causing imaging blurring. As the tilt angle goes higher, the phase shift oscillates between 0 and 2π, with an increasing oscillating frequency. Let's set up an arbitrary criterion that 0.01π (which approximately causes $\frac{\lambda}{100}$ fringe displacement) is the maximum phase shift that will not cause any noticeable image contrast loss. For the case shown in this plot, the maximum tolerable beam tilt angle is 0.15°.

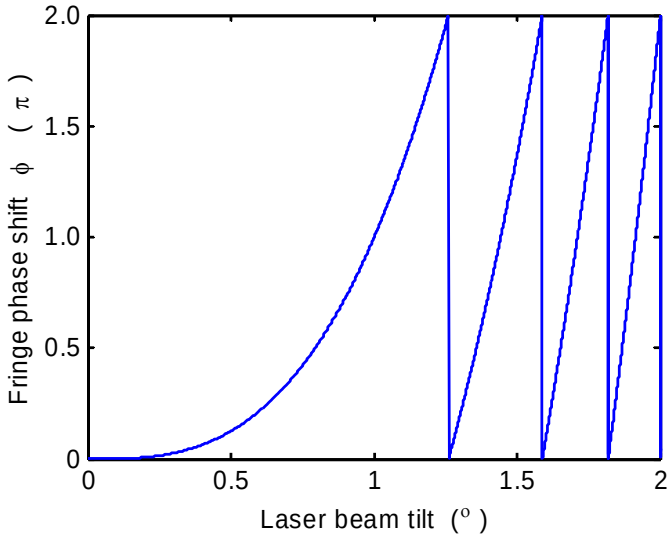

Figure 4. Fringe phase shift ϕ plotted versus laser beam tilt angle. Grating pitch p = 600 nm, setup size D = 10 cm, wavelength λ = 193 nm, $\sin\theta$ = 0.707.

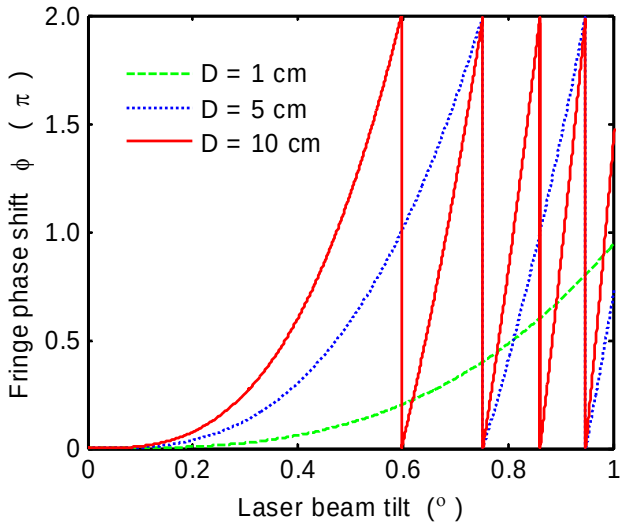

Figure 5. Fringe phase shift ϕ is plotted versus laser beam tilt angle for setup size D= 1 cm, 5 cm, 10 cm respectively. Grating pitch p = 600 nm, wavelength λ = 193 nm, $\sin\theta$ = 0.707.

Setup size D is an important factor determining the phase shift ϕ. In Figure 5, the phase shift due to beam tilt is plotted versus tilt angle at various values of D. It shows that the phase shift due to beam tilt increases as the magnitude of D increases. As a matter of fact, it is a direct proportion relationship, which is indicated in the derivation of Equation [14].

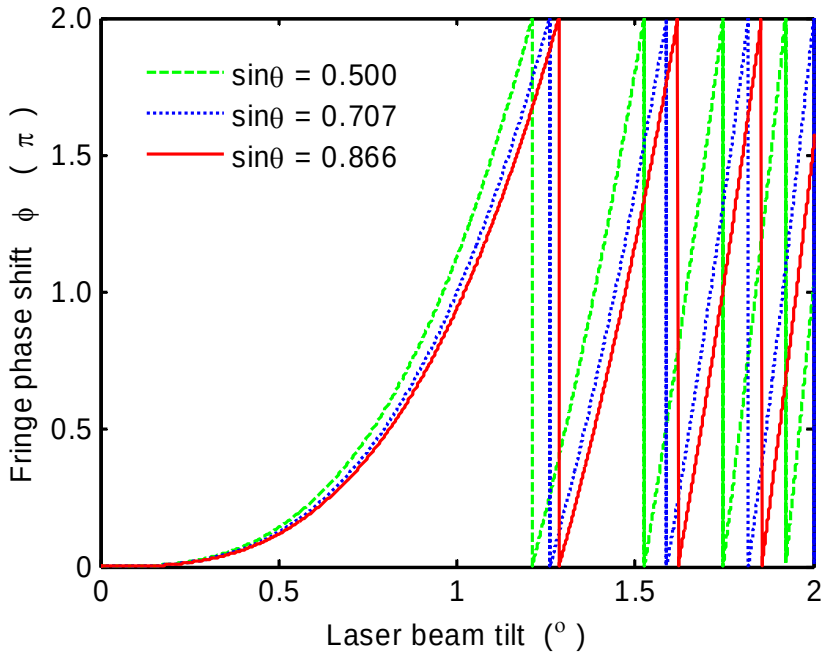

Figure 6. Fringe phase shift ϕ is plotted versus laser beam tilt angle δ for sinθ=0.500, sinθ = 0.707 and sinθ = 0866 respectively. Grating pitch p = 600 nm, wavelength λ = 193 nm.

In Figure 6, the phase shift due to beam tilt is plotted versus tilt angle at various values of interference angle θ. It shows that the phase shift due to beam tilt is relatively non-sensitive to interference angle θ, especially at low tilt angles. This is an important property of the setup. If a certain degree of beam tilt (for example, due to some resonant vibration) does not wash out the fringe patterns at low θ values (i.e., low NA, loose pitches), it is not going to wash out the fringe patterns at high θ values either (i.e., low NA, tight pitches). This property makes it much easier to lay out the vibrations criteria for the interferometric system which is intended to work at various NA values.

In addition to the interference fringe shift (phase shift), laser pointing tilt also could result in change in the pitch of the fringe since the incident angles of the two beams on the wafer plane is a function of the laser tilt angle δ. The change in incident angles in turn induces interference fringe pitch change. As discussed in the proceeding, the incident of angle of the +1st order is θ' and the incident angle of the -1st order is θ'', then the electrical field at the wafer plane can be expressed as,

$$\mathbf{E_1} = |\mathbf{E_1}| e^{-i(kx \sin\theta' + \phi)}$$
$$\mathbf{E_2} = |\mathbf{E_2}| e^{-i(-kx \sin\theta'')} \qquad [15]$$

where $\mathbf{E_1}$ and $\mathbf{E_2}$ are the electrical fields of +1st order and -1st order respectively, k is the propagation vector, and x is the coordinate on the wafer. Following the same method described in reference [10], the total field at the wafer plane in the case of TE polarization can be expressed as,

$$\begin{aligned}\mathbf{E} = \mathbf{E_1} + \mathbf{E_2} &= |\mathbf{E_1}|e^{-i(kx\sin\theta'+\phi)} + |\mathbf{E_2}|e^{-i(-kx\sin\theta'')} \\ &= \left[|\mathbf{E_1}|\cos(kx\sin\theta'+\phi) + |\mathbf{E_2}|\cos(kx\sin\theta'')\right] \\ &\quad - i\left[|\mathbf{E_1}|\sin(kx\sin\theta'+\phi) - |\mathbf{E_2}|\sin(kx\sin\theta'')\right]\end{aligned} \quad [16]$$

The intensity can be derived as,

$$\begin{aligned}I \propto |\mathbf{E}|^2 &= |\mathbf{E_1} + \mathbf{E_2}|^2 \\ &= |\mathbf{E_1}|^2 + |\mathbf{E_2}|^2 + 2|\mathbf{E_1}||\mathbf{E_2}|\cos(kx\sin\theta'+kx\sin\theta''+\phi)\end{aligned} \quad [17]$$

Therefore, the corresponding pitch is,

$$p_{tilt} = \frac{2\pi}{k\sin\theta'+k\sin\theta''} = \frac{\lambda}{n(\sin\theta'+\sin\theta'')} \quad [18]$$

For a laser pointing tilt angle δ, θ' tends to be larger than θ, but θ'' tends to be smaller than θ. For a small tilt angle δ, intuitively, we may think that $\sin\theta'+\sin\theta'' \approx 2\sin\theta$, hence a very small pitch change is expected. To describe the phenomenon quantitatively, let's define a length *L* over which the pitch number difference between the tilted case and non-tilted case is 1,. *L* can be expressed as,

$$L = \frac{1}{\frac{1}{p} - \frac{1}{p_{tilt}}} = \frac{\lambda}{n(2\sin\theta - \sin\theta' - \sin\theta'')} \quad [19]$$

As illustrated in Figure 7, the fringe pattern from tilted beam is out of phase with that from the normal beam at the two ends of length *L*, where the resulted fringe contrast is the worst. If the laser energy is equally distributed between the normal direction and δ-tilt direction, the fringe contrast is zero at those locations. In reality, the contrast will depend on the laser pointing direction statistics. If the length of the desired image area is much smaller than *L*, the contrast loss due to laser pointing instability can be ignored. Therefore, *L* is characteristic of the useful image size that could be obtained in the case of laser pointing instability. Here, it is termed as Tilt Coherence Length.

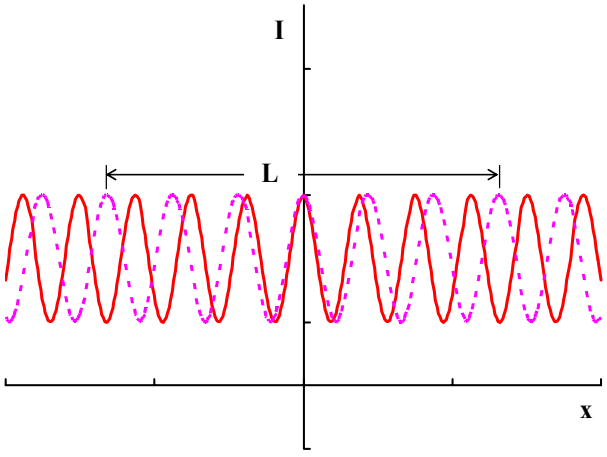

Figure 7. Illustration for interference fringe contrast loss due to fringe pitch change from tilted beam. The solid sinusoidal curve is from normal beam interference and the dashed sinusoidal curve is from tilted beam. Over a length of L, the solid curve has one more number of pitches than that of the dashed curve. At both ends of the length *L*, the contrast is the worst.

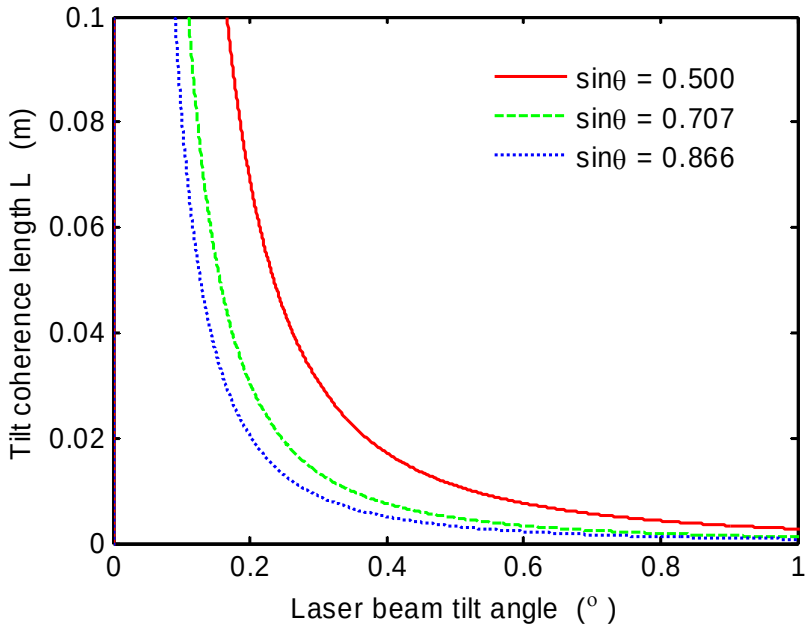

Figure 8. Tilt coherence length is plotted versus laser beam tilt angle. Grating pitch p = 600 nm, setup size D = 1 cm, wavelength λ = 193 nm. sinθ =0.500 (solid curve); sinθ = 0.707 (dashed curve); sinθ = 0.866 (dotted curve).

The tilt coherence length versus laser beam tilt angle is plotted in Figure 8. A grating pitch of $p = 600\,\text{nm}$, setup size of $D = 1\,\text{cm}$ and source wavelength of $\lambda = 193\,\text{nm}$ are used in the calculation. The plots show that the tilt coherence length decreases as the interference angle θ is increased to higher values. It indicates that beam tilt is more sensitive at higher θ values, which lies in our scope of interest. The degree of beam tilt which can be tolerated in our interferometric systems can be derived from the plots if it is the only factor that contributes to fringe contrast loss. In the context that the effective beam size in our setup is around 2~3 mm, a tilt coherence of 200 mm would yield negligible contrast loss. The corresponding tilt angle from the plot is 0.05° in the case of θ = 60° (dotted curve). This would allow us to establish minimum requirements for factors which contribute to beam tilt, such as laser pointing stability, mechanical setup vibration, environmental vibration, etc.

4. BEAM POINTING INSTABILITY WITH GAUSSIAN DISTRIBUTION

The preceding analysis has been focused on one certain laser beam tilt angle. In practice, the laser beam tilt angle has a normal distribution, P(δ), where P is the normal distribution function. The previous has shown that ϕ is directly related to δ, so the distribution of ϕ can be expressed as $P(\delta(\phi))$. Equation [5-17] states that the interference fringe intensity is a function of location x, and tilt angle σ, $I(x, \phi)$. The resultant interference fringe is an average over the values ϕ, that is,

$$I(x) = \int_{-\infty}^{+\infty} I(x,\phi) P(\delta(\phi)) d\phi \quad [20]$$

Substitution of Equation [5-17] gives,

$$I(x) = \int_{-\infty}^{+\infty} \left[|\mathbf{E_1}|^2 + |\mathbf{E_2}|^2 + 2|\mathbf{E_1}||\mathbf{E_2}| \cos(kx \sin\theta' + kx \sin\theta'' + \phi) \right] P(\delta(\phi)) d\phi \quad [21]$$

Assume that σ is very small, then

$$kx \sin\theta' + kx \sin\theta'' = 2kx \sin\theta \quad [22]$$

Equation [5-21] can be rewritten as,

$$I(x) = \int_{-\infty}^{+\infty} \left[|\mathbf{E_1}|^2 + |\mathbf{E_2}|^2 + 2|\mathbf{E_1}||\mathbf{E_2}| \cos(2kx \sin\theta + \phi) \right] P(\delta(\phi)) d\phi \quad [23]$$

Since $P(\delta(\phi))$ is an even function, the above integral is a convolution, which can be simplified as,

$$I(x) = \left\{ |\mathbf{E_1}|^2 + |\mathbf{E_2}|^2 + 2|\mathbf{E_1}||\mathbf{E_2}| \cos(u) \right\} \otimes P(\delta(u)) \quad [24]$$

where $u = 2kx \sin\theta$. Evaluation of the above convolution yields,

$$I(x) = |\mathbf{E_1}|^2 + |\mathbf{E_2}|^2 + 2\Im\{P(\delta(u))\}\Big|_{\frac{1}{2\pi}} |\mathbf{E_1}||\mathbf{E_2}| \cos(u) \quad [25]$$

where $\Im\{P(\delta(u))\}\Big|_{\frac{1}{2\pi}}$ is the Fourier transform of $P(\delta(u))$ evaluated at $\frac{1}{2\pi}$. The contrast of the fringe can be expressed as,

$$\text{Contrast} = 2\Im\{P(\delta(u))\}\Big|_{\frac{1}{2\pi}} \frac{|\mathbf{E_1}||\mathbf{E_2}|}{|\mathbf{E_1}| + |\mathbf{E_2}|} \quad [26]$$

If the two beams are equal in intensity, the contrast can be reduced as,

$$\text{Contrast} = \Im\{P(\delta(u))\}\Big|_{\frac{1}{2\pi}} \quad [27]$$

If the standard deviation σ of beam direction fluctuation is known, that is, P(δ) is known, it allows us to numerically evaluate the fringe contrast in the absence of laser beam direction fluctuation. An example is shown in Figure 9.

In this figure, the fringe contrast is plotted versus the standard deviation σ of beam direction fluctuation. Configuration size D=0.01m, interference angle θ=45°, wavelength λ=193nm and grating pitch=600nm are used in the calculation. The simulation results show that the contrast drops rapidly at σ=0.5°. The excimer laser used for lithography has an intrinsic σ of about 20μ radians,[9] the effect of which on interference fringe contrast can be ignored, as shown in Figure 9. In addition to intrinsic laser pointing instability, other factors such mechanical resonant vibration, environmental vibration, etc. might bring the standard deviation σ of the beam direction fluctuation to a higher value. Under those circumstances, the contrast loss of the interference fringe is well described by the curve in Figure 9.

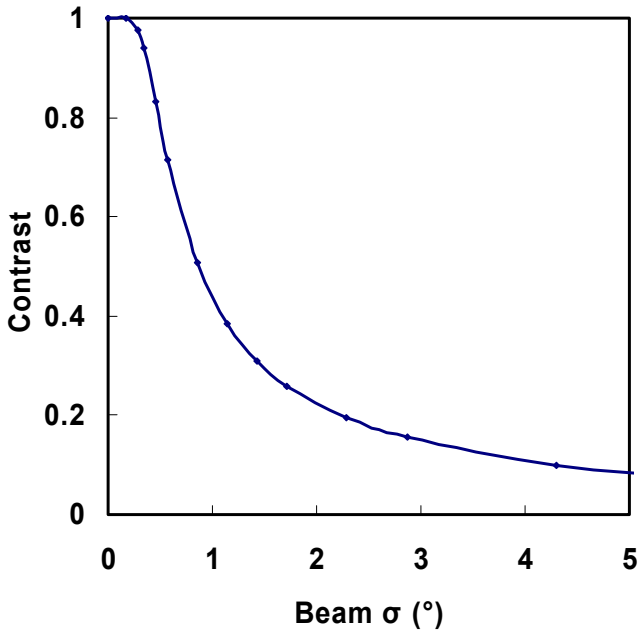

Figure 9. Interference fringe contrast is plotted versus the standard deviation σ of beam direction fluctuation. D=0.01m, sinθ=0.707, λ=193nm, grating pitch=600nm, TE polarization.

5. CONCLUSION

Using geometrical ray tracing technique and basic interference theory, the effects of beam pointing instability on the contrast of interference fringe were analyzed for a two-beam interferometric lithography setup described in this paper. The established relationship between beam tilt angle and interference fringe displacement allows the evaluation of the fringe contrast if the beam pointing direction is not stable during the exposure. The analysis shows that a setup configuration with smaller size is more tolerant with beam pointing instability. It also shows that the system is more tolerant with beam pointing instability at higher interference angles. For a beam pointing instability with random distribution, it has been shown that, the resulted fringe contrast is directly proportional to the Fourier transform of the beam pointing direction distribution evaluated at $\frac{1}{2\pi}$. A numerical simulation example was given for a beam pointing direction with normal distribution. The example shows that a beam pointing direction of Gaussian distribution with standard deviation less than 0.25 degree does not noticeably affect the contrast of the resulted interference fringe. The analysis introduced in this paper may be applied to evaluate any factors contributing to beam direction fluctuation, such as intrinsic laser pointing instability, mechanical resonant vibration, environmental vibration, etc.

6. REFERENCES

1. B. W. Smith, “Optics for Photolithography,” in *Microlithography Science and Technology*, J. R. Sheats, B. W. Smith, eds. (Marcel Dekker, 1998) , pp171-270.

2. D. G. Flagello, T. D. Milster, "High-numerical-aperture effects in photoresist", *Applied Optics*, **36**, 8944-8951 (1997)
3. D. G. Flagello, T. D. Milster, A. E. Rosenbluth, "Theory of high-NA imaging in homogeneous thin films", *J. Opt. Soc. Am. A*, **13**, 53-64 (1999).
4. A. K. Raub, S. R. Brueck, "Deep-UV immersion interferometric lithography", in *Optical Microlithography XVI*, A. Yen ed., Proc. SPIE , **5377**, 306-318 (2003).
5. A. K. Raub, A. Frauenglass, S. R. Brueck, W. Conley, R. R. Dammel, A. Romano, M. Sato, W. Hinsberg, "Deep-UV immersion interferometric lithography", in *Optical Microlithography XVII*, B. W. Smith ed., Proc. SPIE , **5377**, 306-318 (2004).
6. F. Cropanese, A. Bourov, Y. Fan, A. Estroff, L. Zavyalova, "Synthesis of projection lithography for low k1 via interferometry", in *Optical Microlithography XVII*, B. W. Smith ed., Proc. SPIE , **5377**, PART 3, 1836-1842 (2004).
7. A. Bourov, Y. Fan, F. C. Cropanese, N. V. Lafferty, L. V. Zavyalova, H. Kang, B. W. Smith, "Immersion microlithography at 193 nm with a Talbot prism interferometer", in *Optical Microlithography XVII*, B. W. Smith ed., Proc. SPIE , **5377**, PART 3, 1573-1578 (2004).
8. B. W. Smith, A. Bourov, Y. Fan, F. Cropanese, P. Hammond, "Amphibian XIS: an immersion lithography microstepper platform", ", in *Optical Microlithography XVIII*, B. W. Smith ed., Proc. SPIE , **5754**, 751-759 (2005).
9. R. F. Delmdahl, "Pulsed excimer lasers for thin film applications", in *Fifth International Symposium on Laser Precision Microfabrication*, Proc. SPIE , 5662, PART 1, 655-660 (2004).
10. Y. Fan, A. Bourov, L. Zavyalova, J. Zhou, A. Estroff, N. Lafferty, B. W. Smith, "ILSim: a compact simulation tool for interferometric lithography", in *Optical Microlithography XVIII*, B. W. Smith ed., Proc. SPIE , **5754**, 1805-1816 (2005).